

# Compatibility of DAMA Dark Matter Detection with Other Searches

Paolo Gondolo<sup>1</sup> and Graciela Gelmini<sup>2</sup>

<sup>1</sup> *Department of Physics, University of Utah, 115 S 1400 E # 201, Salt Lake City, UT 84112, USA*

<sup>2</sup> *Department of Physics and Astronomy, UCLA, 405 Hilgard Ave. Los Angeles, CA 90095, USA*

paolo@physics.utah.edu, gelmini@physics.ucla.edu

(Dated: April 1, 2005)

We present two examples of velocity distributions for light dark matter particles that reconcile the annual modulation signal observed by DAMA with all other negative results from dark matter searches. They are: (1) a conventional Maxwellian distribution for particle masses around 5 to 9 GeV; (2) a dark matter stream coming from the general direction of Galactic rotation (not the Sagittarius stream). Our idea is based on attributing the DAMA signal to scattering off Na, instead of I, and can be tested in the immediate future by detectors using light nuclei, such as CDMS-II (using Si) and CRESST-II (using O).

PACS numbers: 95.35.+d

The nature of dark matter is one of the fundamental problems of physics and cosmology. Popular candidates for dark matter are weakly interacting massive particles (WIMPs). Direct searches for dark matter WIMPs aim at detecting the scattering of WIMPs off of nuclei in a low-background detector. These experiments measure the energy of the recoiling nucleus, and are sensitive to a signal above a detector-dependent energy threshold [1].

One such experiment, the DAMA collaboration [2], has found an annual modulation in its data compatible with the signal expected from dark matter particles bound to our galactic halo [3]. Other such experiments, such as CDMS [4, 5], EDELWEISS [6, 7], and CRESST [8, 9], have not found any signal from WIMPs. It has been difficult to reconcile a WIMP signal in DAMA with the other negative results [10].

Here we show that it is possible to have a dark matter signal above the WIMP speed threshold for DAMA and below the WIMP speed threshold for CDMS and EDELWEISS, so that the positive and negative detection results can be compatible. We find: (1) that with the standard dark halo model there is a solution for WIMP masses about 6-9 GeV and WIMP-proton scattering cross section of about 1 femtobarn ( $10^{-39}$  cm<sup>2</sup>), and (2) that this region of solutions can be enlarged if a dark matter stream is suitably added to the standard dark halo. The region in point (1) could certainly also be enlarged by considering more general halo models, even in the absence of dark matter streams (see e.g. the models in [11]).

Light neutralinos as WIMPs with masses as low as 2 GeV [12] or, with updated bounds, 6 GeV [13] have been considered, but their cross sections are about one order of magnitude smaller than those needed here. In this paper we proceed in a purely phenomenological way in choosing the WIMP mass and cross section, although we concentrate on spin-independent cross sections only. We do not attempt to provide an elementary particle model to support the values of masses and cross sections. As justification of our approach, let us recall that there is no proven particle theory of dark matter. The candidates we are considering are stable neutral particles which have very small cross sections with nucleons, of the order of femtobarns. Regarding their production in accelerators, they would escape from the detectors without interacting. Unless there is a concrete specific model relating our neutral candidate to other charged particles (which yes can be observed) there is no way such particles could be found in accelerators. The usual signature searched for in accelerators, for example at LEP, Tevatron or LHC, is the emission of a charged particle related to the neutral particle in question. For example, searching for “neutralinos” one puts bounds on one of its cousins, a “chargino”, or another relative, a “slepton”. Without a detailed model there are no accelerator bounds on neutral dark matter candidates.

## II. BASIC IDEA

Our idea is that WIMPs with velocities smaller than the CDMS threshold but larger than the DAMA threshold could explain the data. Our idea is based on the following observation.

The minimum WIMP speed required to produce a nuclear recoil energy  $E$  is given by elementary kinematics as

$$v = \sqrt{\frac{ME}{2\mu^2}} = \sqrt{\frac{(m+M)^2 E}{2Mm^2}}. \quad (1)$$

Here  $\mu = mM/(m+M)$  is the reduced WIMP-nucleus mass,  $m$  is the WIMP mass and  $M$  is the nucleus mass.

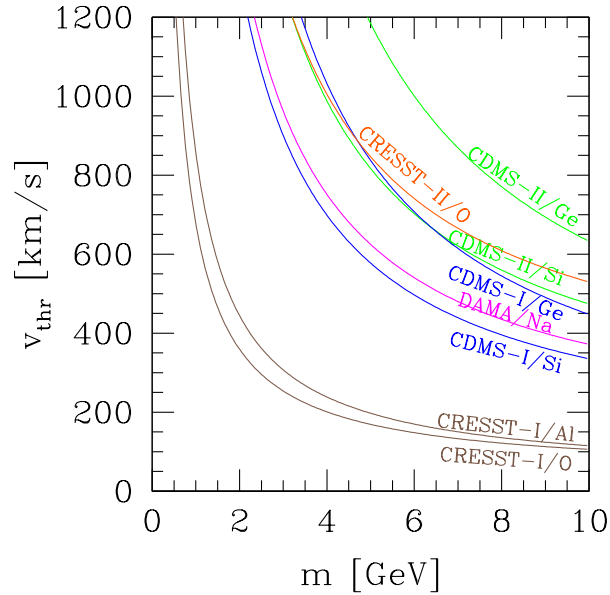


FIG. 1: Threshold speeds  $v_{\text{thr}}$  of several experiments and target nuclei. The DAMA Na threshold is lower than the CDMS-I Ge threshold for  $m < 22.3$  GeV.

The nuclear energy threshold  $E_{\text{thr}}$  observable with a particular nucleus corresponds through Eq. (1) to a minimum observable WIMP speed, the speed threshold  $v_{\text{thr}}$ . Speed thresholds for several direct detection experiments listed in Table 1 are plotted in Fig. 1 as a function of the WIMP mass in the range  $m < 10$  GeV. Using Eq. (1), it is easy to see that the speed threshold of Na in DAMA is smaller than that of Ge in CDMS-I for  $m < 22.3$  GeV.

To understand the dependence of the speed threshold on nuclear mass, consider the simple case  $m \ll M$ . Then  $\mu \simeq m$  is independent of the nucleus mass  $M$ , and  $v_{\text{thr}}$  is proportional to  $\sqrt{ME_{\text{thr}}}$ . Using the nuclear masses of Na and Ge,  $M_{\text{Na}} = 21.41$  GeV and  $M_{\text{Ge}} = 67.64$  GeV, and the energy thresholds in Table 1, the product  $ME_{\text{thr}}$  is smaller for Na in DAMA than for Ge in CDMS-I (notice that DAMA used “electron-equivalent” energies, which we indicate with keVee units; these need to be converted into nucleus recoil energies using the so-called quenching factors listed in the caption of Table 1). For  $m \ll M$ , the Ge  $v_{\text{thr}}$  in CDMS-I is 2.44 times the Na  $v_{\text{thr}}$  in DAMA.

For  $m$  not necessarily much smaller than  $M$ , we can refer to Fig. 1. The speed threshold of Ge in CDMS-I, of Si and Ge in CDMS-II, of Ge in EDELWEISS, as well as those of other experiments using heavier nuclei, are larger than the speed threshold of Na in DAMA in the WIMP mass range shown. Three light nuclei, namely Si in CDMS and Al and O in CRESST, have speed thresholds lower than Na in DAMA, and can be used to test and constrain our idea.

A small component of Si is present in CDMS. Si is lighter than Ge, although heavier than Na,  $M_{\text{Si}} = 26.16$  GeV. Given the nuclear energy recoil thresholds in Table 1, the speed threshold of Si in CDMS-I is smaller than that of Na in DAMA for all WIMP mass values. However, considering the CDMS-I efficiency close to 5 keV energies is about 8%, the effective exposure of the CDMS-I Si detector near threshold is about 0.5 kg-day, which may be too small to have detected the signal which DAMA might have seen in its Na detector. In any event, CDMS has not yet used its Si component to set limits on dark matter, but only to help in background rejection.

Light nuclei are used by CRESST, in particular O ( $M_{\text{O}} = 14.90$  GeV). CRESST-I [8] used sapphire ( $\text{Al}_2\text{O}_3$ ), which besides O contains Al, similar in mass to Si. CRESST-I has set limits on dark matter with a very low nuclear recoil threshold of 0.6 keV, but with a small exposure of only 1.5 kg-day. The speed threshold for O in CRESST-I is so low that CRESST-I is sensitive to the bulk of the halo dark matter particles we are proposing. CRESST-II uses calcium tungstate ( $\text{CaWO}_4$ ), which also contains the light O nucleus, but background discrimination sets a relatively high threshold of  $\sim 10$  keV. CRESST-II has run a prototype without neutron shield and set the limits quoted in Table 1 [9]. The completed CRESST-II will test our idea.

In summary, for light enough WIMPs it could be possible to have dark matter WIMPs with a speed above threshold for Na in DAMA, and below threshold for Ge in CDMS and EDELWEISS. That is, we could have a dark matter signal visible for DAMA but not observable in CDMS and EDELWEISS and compatible with all experimental data.

Experiment	Exposure [kg-day]	Threshold [keV]	Efficiency [%]	Constraint	Ref.
CDMS-I	Si: 6.58 Ge: 65.8	5	$E < 10\text{keV: } 7.6$ $E < 20\text{keV: } 22.8$ $E > 20\text{keV: } 38$	5–55keV: <2.3 events (†)	[4]
CDMS-II	Si: 5.26 Ge: 52.6	10	$E < 20\text{keV: } 22.8$ $E > 20\text{keV: } 38$	10–100keV: <2.3 events (†)	[5]
EDELWEISS	Ge: 8.2 (⊗)	20	100	20–100keV: <2.3 events (†)	[6]
CRESST-I	Al <sub>2</sub> O <sub>3</sub> : 1.51	0.6	100	(‡)	[8]
CRESST-II	CaWO <sub>4</sub> : 10.448	10	100	Ca+O, 15–40keV: <6 events W, 12–40keV: <2.3 events (†)	[9]
DAMA/NaI-96	NaI: 4123.2	I: 22 (◇) Na: 6.7 (◇)	100	1–2keVee: <1.4/kg-day-keVee (★) 2–3keVee: <0.4/kg-day-keVee (★)	[14]
DAMA/NaI-03	NaI: 107731	I: 22 (◇) Na: 6.7 (◇)	100	2–4keVee: $0.0233 \pm 0.0047$ /kg-day-keVee (●) 2–5keVee: $0.0210 \pm 0.0038$ /kg-day-keVee (●) 2–6keVee: $0.0192 \pm 0.0031$ /kg-day-keVee (●) 6–14keVee: $-0.0009 \pm 0.0019$ /kg-day-keVee (●)	[11]

TABLE I: Experimental constraints used in this study. Notes to the table: (†) upper limit assuming no detected event; (⊗) final EDELWEISS-I results [7] with 62 kg-days exposure do not give more stringent bounds because 59 events, attributed to background, have been detected between 10 and 200 keV; (‡) to reproduce the published curve in [8], we impose appropriate upper limits all along the recoil spectrum in their Fig. 1; (◇) from an electron equivalent threshold of 2 keVee, using the quenching factors  $Q = E_{ee}/E$  equal to 0.09 for I and 0.3 for Na [11]; (★) approximations that reproduce the published  $\sigma_p$  vs.  $m$  limit across our mass range; (●) amplitude of annual modulation from the model-independent fit in [11] assuming a period of 1 yr and the maximum counting rate at June 2.

### III. METHOD

Our procedure is the following. Given a dark halo model, including the WIMP velocity distribution, we find the viable region by making sure that we produce the correct amplitude for the DAMA modulation in the viable region and that all of the current experimental constraints are satisfied.

We consider constraints from DAMA/NaI-96 [14], DAMA/NaI-03 [11], EDELWEISS [6], CDMS-I [4], CDMS-II [5], CRESST-I [8], and CRESST-II [9]. The experimental exposures, efficiencies, thresholds, and constraints we use are listed in Table 1.

To compute the number of recoil events in a given detector we start by defining the effective exposure of each nuclear species  $i$  in the detector (expressed in kg-days of isotope  $i$ ) as

$$\mathcal{E}_i = \mathcal{M}_i T_i \epsilon_i(E), \quad (1)$$

where  $T_i$  is the active time of the detector during which a mass  $\mathcal{M}_i$  of nuclei of species  $i$  is exposed to the signal, and  $\epsilon_i(E)$  is the counting efficiency for nuclear recoils of energy  $E$  (for the counting efficiency we assume the values in Table 1). Then the expected number of recoil events with recoil energy in the range  $(E_1, E_2)$  is the following sum over the nuclear species in the detector,

$$N_{E_1-E_2} = \sum_i \int_{E_1}^{E_2} \frac{dR_i}{dE} \mathcal{E}_i(E) dE. \quad (2)$$

Here  $dR_i/dE$  is the expected recoil rate per unit mass of species  $i$  per unit nucleus recoil energy and per unit time. It is

$$\frac{dR_i}{dE} = \frac{\rho \sigma_i |F_i(E)|^2}{2m\mu_i^2} \int_{v > \sqrt{M_i E/2\mu_i^2}} \frac{f(\mathbf{v}, t)}{v} d^3v. \quad (3)$$

In Eq. (3),  $M_i$  is the mass of a nucleus of species  $i$ ,  $m$  is the WIMP mass,  $\mu_i = mM_i/(m + M_i)$  is the reduced WIMP-nucleus mass,  $\rho$  is the local halo WIMP density,  $F_i(E)$  is a nuclear form factor for species  $i$  (see below),  $\sigma_i$  is the WIMP-nucleus cross section,  $\mathbf{v}$  is the velocity of the WIMP with respect to the detector,  $v = |\mathbf{v}|$ , and  $f(\mathbf{v}, t)$  is the WIMP velocity distribution in the reference frame of the detector.

In this analysis, we assume that the WIMP-nucleus interaction is spin-independent. We make the usual assumption [1] that the cross section  $\sigma_i$  scales with the square of the nucleus atomic number  $A_i$ . Thus, in terms of the WIMP-proton cross section  $\sigma_p$ , the scaling is  $\sigma_i = \sigma_p A_i^2 (\mu_i/\mu_p)^2$ . For the nuclear form factor we use the conventional Helm form [1],  $F_i(E) = 3e^{-q^2 s^2/2} [\sin(qr) - qr \cos(qr)] / (qr)^3$ , with  $s = 1$  fm,  $r = \sqrt{R^2 - 5s^2}$ ,  $R = 1.2A_i^{1/3}$  fm,  $q = \sqrt{2M_i E}$ .

A technical point: DAMA obtains the nuclear recoil energy  $E$  not directly but as a multiple of a measured electron-equivalent energy  $E_{ee} = QE$ . The quenching factor  $Q$  depends on the nuclear target and has been found experimentally [11] to have the values  $Q_{\text{Na}} = 0.3$  and  $Q_{\text{I}} = 0.09$ . DAMA results are quoted in electron-equivalent energy (keVee), and Eq. (2) needs to be modified to

$$N_{E_{ee,1}-E_{ee,2}} = \sum_i \int_{E_{ee,1}/Q_i}^{E_{ee,2}/Q_i} \frac{dR_i}{dE} \mathcal{E}_i(E) dE. \quad (4)$$

The time dependence of the WIMP distribution function  $f(\mathbf{v}, t)$  is due to the revolution of the Earth around the Sun [3]. This gives rise to a modulation in the expected counting rate with a period of a year. For a conventional halo, the counting rate varies approximately sinusoidally [3], while for other halo models, in particular for models with streams, the time dependence is in general not sinusoidal [20]. We define the amplitude of the annual modulation as half of the difference between maximum and minimum counting rates. Explicitly, for the  $(E_{ee,1}, E_{ee,2})$  electron-equivalent energy interval in DAMA, the modulation amplitude in counts/kg-day-keVee is

$$\mathcal{A}_{E_{ee,1}-E_{ee,2}} = \frac{1}{2} \left[ \mathcal{R}_{E_{ee,1}-E_{ee,2}}^{\max} - \mathcal{R}_{E_{ee,1}-E_{ee,2}}^{\min} \right], \quad (5)$$

where  $\mathcal{R}_{E_{ee,1}-E_{ee,2}}^{\max}$  and  $\mathcal{R}_{E_{ee,1}-E_{ee,2}}^{\min}$  are the maximum and minimum values of the counting rate during the course of a year per kg-day-keVee

$$\mathcal{R}_{E_{ee,1}-E_{ee,2}} = \frac{1}{\mathcal{E}_{\text{DAMA}}} \frac{N_{ee,2} - N_{ee,1}}{E_{ee,2} - E_{ee,1}}. \quad (6)$$

Here  $\mathcal{E}_{\text{DAMA}} = (\mathcal{M}_{\text{Na}} + \mathcal{M}_{\text{I}})T$  is the DAMA exposure as listed in Table 1.

We need to fix the WIMP velocity distribution. In this paper we consider either a conventional Maxwellian distribution or the conventional Maxwellian distribution plus a dark matter stream (we discuss these two choices separately in the next sections).

In both cases, we proceed to vary the WIMP mass and the parameters in the velocity distribution. For each choice of these variables we find the range of WIMP-proton cross sections  $\sigma_p$  that produce the desired modulation amplitude  $\mathcal{A}$  in DAMA/NaI at the  $3\sigma$  or 90% confidence level. In detail, let  $\mathcal{A}_{2-6}$  be the expected modulation in the 2-6 keVee bin of DAMA/NaI-03, as computed using Eq. (5), and let  $\mathcal{A}_{2-6}^{\text{DAMA}} \pm \delta\mathcal{A}_{2-6}^{\text{DAMA}}$  be the model-independent experimental fit to the annual modulation amplitude with a fixed period of 1 yr and maximum rate June 2, as provided by the DAMA collaboration in [11] and listed in Table 1 (i.e.  $\mathcal{A}_{2-6}^{\text{DAMA}} \pm \delta\mathcal{A}_{2-6}^{\text{DAMA}} = 0.0233 \pm 0.0047$  counts/kg-day-keVee). Analogously, define the quantities  $\mathcal{A}_{6-14}$  and  $\mathcal{A}_{6-14}^{\text{DAMA}} \pm \delta\mathcal{A}_{6-14}^{\text{DAMA}}$  for the 6-14 keVee energy bin. To find the best-fit value of  $\sigma_p$  we minimize the quantity

$$\chi^2 = \left( \frac{\mathcal{A}_{2-6} - \mathcal{A}_{2-6}^{\text{DAMA}}}{\delta\mathcal{A}_{2-6}^{\text{DAMA}}} \right)^2 + \left( \frac{\mathcal{A}_{6-14} - \mathcal{A}_{6-14}^{\text{DAMA}}}{\delta\mathcal{A}_{6-14}^{\text{DAMA}}} \right)^2. \quad (7)$$

This gives us  $\chi_{\min}^2$  and  $\sigma_{p,\min}$ . We accept the value  $\sigma_{p,\min}$  only if

$$\chi_{\min}^2 < 2. \quad (8)$$

Then we determine an  $n\sigma$  confidence interval for  $\sigma_p$  by imposing that  $\Delta\chi^2 = \chi^2(\sigma_p) - \chi_{\min}^2$  satisfies

$$\Delta\chi^2 < n^2, \quad (9)$$

and a 90% confidence interval by imposing that

$$\Delta\chi^2 < 2.71. \quad (10)$$

These are the appropriate values of  $\Delta\chi^2$  for two data points ( $\mathcal{A}_{2-6}$  and  $\mathcal{A}_{6-14}$ ) and one parameter ( $\sigma_p$ ) (see, e.g., the Statistics Section in [15]).

We have also replaced the 2-6 keVee bin with the 2-4 keVee bin. One obtains larger regions of  $\sigma_p$  satisfying our condition. Since the 2-4 and 2-6 keVee bins are correlated, we show results for both.

Our procedure differs from previous theoretical analyses [10] in that we use the modulation amplitudes provided by DAMA in their model-independent analysis [11] instead of their best-fit values obtained fixing the shape of the nuclear recoil spectrum to that appropriate for the conventional halo model [14]. The latter best-fit values depend on

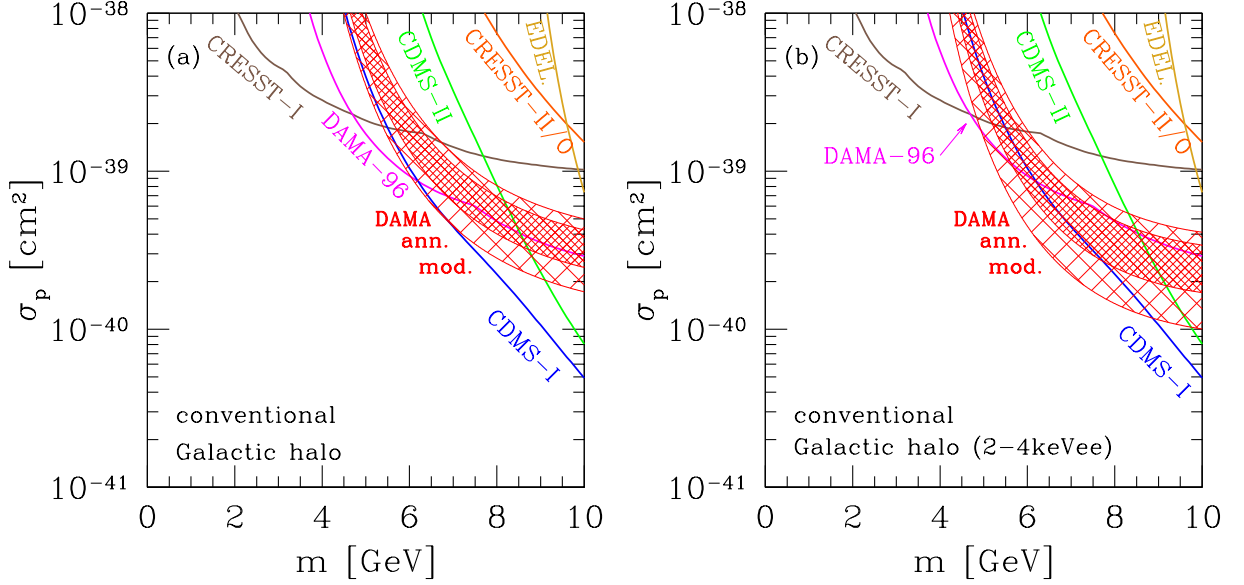


FIG. 2: Comparison of the DAMA annual modulation region with other direct detection bounds for spin-independent WIMP-proton interactions and a conventional dark halo. In (a) the 2-6 and 6-14 keV DAMA bins and in (b) the 2-4 and 6-14 keV DAMA bins were used. In the hatched region, the WIMP-proton cross section  $\sigma_p$  at WIMP mass  $m$  reproduces the DAMA annual modulation results at the 90% and  $3\sigma$  C.L. (inner densely hatched region and outer hatched region, respectively). The region above each other line is excluded at 90% C.L. by the corresponding experiment (DAMA/NaI-96, CRESST-I and II, EDELWEISS, and CDMS-I and II). In (a), there is a region compatible with the DAMA annual modulation and all other experiments at the  $3\sigma$  but not the 90% C.L. In (b), there is a compatible region at the 90% C.L. also.

the conventional recoil spectrum at the specific best-fit WIMP mass of DAMA ( $52^{+10}_{-8}$  GeV). Thus we must use the model-independent fit to consider different WIMP masses and non-conventional halo models.

Having found a WIMP-proton cross section that produces the DAMA annual modulation at  $n$ -sigma (or 90%) confidence, we evaluate the expected number of events in all of the other experiments using Eq. (2), and compare them with the constraints in Table 1. We require that less than 2.3 events are predicted for each experiment that observes no events (this is the 90% C.L. upper bound). All other upper bounds in Table 1 are also at 90% C.L. We thus determine if the parameters we choose are compatible with all the experimental constraints we impose.

We take an additional step in the case in which a dark matter stream is added to the conventional halo model. After having followed the procedure described so far, we determine the minimum and maximum values of the WIMP mass for which there is a (part of the)  $\sigma_p$  confidence interval that produces the DAMA annual modulation and is allowed by all other experiments at 90% C.L.

#### IV. CONVENTIONAL HALO MODEL

Since the experimental bounds on the candidate mass and cross section depend on the halo model adopted, all dark matter direct detection experiments conventionally adopt the same isothermal halo model, to be able to compare their results. In this section, we adopt the same conventional halo model, so as not to innovate in this respect. We make no claim that this is a realistic halo model, but it offers us a definite benchmark for comparison.

The value of the local WIMP density conventionally adopted in direct detection comparisons is  $\rho = 0.3$  GeV/cm<sup>3</sup>. This we adopt.

The conventional WIMP velocity distribution used in the comparison of direct detection experiments is a Maxwellian distribution truncated at the local Galactic escape speed  $v_{\text{esc}}$ . In the reference frame of the detector, which we take to coincide with the reference frame of the Earth, the conventional WIMP velocity distribution reads

$$f_h(\mathbf{v}, t) = \begin{cases} \frac{1}{N_h(2\pi\sigma_h^2)^{3/2}} e^{-|\mathbf{v} + \mathbf{v}_\odot + \mathbf{v}_\oplus(t)|^2/2\sigma_h^2} & \text{if } |\mathbf{v} + \mathbf{v}_\odot + \mathbf{v}_\oplus(t)| < v_{\text{esc}}, \\ 0 & \text{otherwise.} \end{cases} \quad (1)$$

Here  $\mathbf{v}$  is the velocity of a WIMP relative to the Earth,  $\mathbf{v}_{\oplus}(t)$  is the velocity of the Earth relative to the Sun, and  $\mathbf{v}_{\odot}$  is the velocity of the Sun relative to the Galactic rest frame, with respect to which the halo WIMPs are assumed to be stationary. Moreover,  $\sigma_h$  is the velocity dispersion of the WIMPs, and  $N_h = \text{erf}(z/\sqrt{2}) - (2/\pi)^{1/2} z e^{-z^2/2}$ , with  $z = v_{\text{esc}}/\sigma_h$ , is a normalization factor.

For  $\mathbf{v}_{\oplus}(t)$ , we assume a magnitude of 29.8 km/s and a direction tangent to a circular orbit on the ecliptic plane.

For  $\mathbf{v}_{\odot}$ , we assume the conventional value adopted in our field, namely 232 km/s in the direction with ecliptic coordinates  $\lambda_{\odot} = 340^\circ$ ,  $\beta_{\odot} = 60^\circ$ .<sup>1</sup>

We set the velocity dispersion to the conventional value  $\sigma_h = 220/\sqrt{2}$  km/s (as applies to an isothermal model), and we take the escape speed from the galaxy to be  $v_{\text{esc}} = 650$  km/s. With the halo model we assume, the maximum possible heliocentric velocity of a halo particle is  $v_{\text{esc}} + v_{\odot} = 882$  km/s.

Following the procedure discussed in Section III, we obtain the results in Figs. 2(a-b). In these figures we show all the experimental bounds on the WIMP-proton cross section and mass that we obtain using the content of Table 1, together with the region where the DAMA modulation is well reproduced at the 90% C.L. (denser central hatched region) and  $3\sigma$  C.L. (hatched region). Figs. 2(a) and 2(b) show the DAMA region obtained by using their 2-6 and 6-14 keVee data bins (Fig. 2a) and their 2-4 and 6-14 keVee data bins (Fig. 2b). Also shown are the regions excluded by the experiments in Table 1 (DAMA/NaI-96, CRESST-I and II, EDELWEISS, and CDMS-I and II). In Fig. 2(a), there is a region compatible with the DAMA annual modulation and all other experiments at the  $3\sigma$  but not the 90% C.L. (notice that the experimental bounds are at the 90% C.L. and would be less stringent at the  $3\sigma$  level). In Fig. 2(b), there is a compatible region at the 90% C.L. also. Since the 2-4 and 2-6 keVee data bins are correlated, we do not have a means of saying if using one or the other is better. Thus we conclude that the agreement of DAMA with all other experiments is marginal when using the standard halo model. This means, though, that we expect a larger, more convincing, region of compatibility between DAMA and all the other experiments if the halo model is extended beyond the conventional model, for example using the models in Ref. [11] or, as presented in the next section, introducing additional components to the dark halo, such as a dark matter stream.

## V. ADDITIONAL DARK MATTER STREAM

In this section, we add a stream of dark matter to the conventional halo model. In this we follow the spirit of [18, 19, 20, 21], but look for a stream with velocity above threshold for Na in DAMA and below threshold for Ge in CDMS. Although the stream gives the dominant signal in DAMA (because there are few halo WIMPs above the DAMA threshold), the signal due to the bulk of the halo (e.g. in CRESST) is not significantly affected.

We include the dark matter stream by letting the WIMP velocity distribution be the sum of the conventional velocity distribution  $f_h(\mathbf{v}, t)$  of the previous section and a contribution from the dark matter stream  $f_{\text{str}}(\mathbf{v}, t)$ ,

$$f(\mathbf{v}, t) = f_h(\mathbf{v}, t) + f_{\text{str}}(\mathbf{v}, t). \quad (1)$$

For the stream contribution, we assume a Gaussian function stationary relative to the stream and with velocity dispersion  $\sigma_{\text{str}}$ . In the Earth reference frame, the stream velocity distribution is

$$f_{\text{str}}(\mathbf{v}, t) = \frac{\xi_{\text{str}}}{(2\pi\sigma_{\text{str}}^2)^{3/2}} e^{-|\mathbf{v} - \mathbf{v}_{\text{str}} + \mathbf{v}_{\oplus}(t)|^2 / 2\sigma_{\text{str}}^2}. \quad (2)$$

Here  $\xi_{\text{str}}$  is the local dark matter density in the stream (in units of the mean local halo density  $\rho = 0.3$  GeV/cm<sup>3</sup>),  $\mathbf{v}$  is the velocity of the WIMP relative to the Earth,  $\mathbf{v}_{\oplus}(t)$  is the velocity of the Earth relative to the Sun, and  $\mathbf{v}_{\text{str}}$  is the velocity of the stream relative to the Sun (heliocentric velocity).

We fix the stream velocity dispersion  $\sigma_{\text{str}} = 20$  km/s. Factor-of-2 variations of this value lead to small changes in the results. We consider stream density fractions  $\xi_{\text{str}}$  of up to 3%. Detailed studies of the evolution of possible residual substructure in the galactic dark halo concluded that there is a high probability for the Earth to be passing through a dark matter clump or stream with density  $\sim 3\%$  of the mean local halo density [21]. Ref. [21] studied mostly clumps that have orbited the Galaxy between one and four times (although mentioning that clumps that have orbited the Galaxy more times can also produce cold, high velocity streams in the solar neighborhood) and found

---

<sup>1</sup> This velocity of the Sun in the Galactic rest frame is conventional in our field. It consists of the IAU recommended value of 220 km/s for the galactic rotation speed plus the proper motion of the Sun. In reality, estimates of the local galactic rotation speed range from 170 km/s to 250 km/s (see e.g. [16]) and the Sun's proper motion is subject to statistical and systematic errors of the order of 10 km/s.

plausible clump velocities relative to Earth of 400 to 700 km/s and velocity dispersions of 20 to 50 km/s. The dark matter stream may also be of extragalactic origin. We comment about this possibility later.

Instead of the direction of  $\mathbf{v}_{\text{str}}$ , we specify the ecliptic coordinates  $(\lambda_{\text{str}}, \beta_{\text{str}})$  of the arrival direction of the stream, i.e. the direction of  $-\mathbf{v}_{\text{str}}$ . This we do to be able to compare directly with the arrival direction in the conventional halo model, which is the direction of motion of the Sun in the Galactic rest frame  $(\lambda_{\odot}, \beta_{\odot}) = (340^\circ, 60^\circ)$ .

In order to account for the DAMA annual modulation, the stream arrival direction is limited by the requirement that the DAMA modulation peaks May  $21 \pm 22$  days. To find the direction of the Earth velocity at that time, we reason as follows. May 21 is 61 days after the Spring equinox (March 21), and thus the Sun is at ecliptic longitude  $61/365.25 \times 360 = 60^\circ$ . Since the radius vector to the Sun and the velocity of the Earth are almost perpendicular (they are exactly so for a circular orbit), May 21 the Earth is moving toward a point of ecliptic longitude  $60^\circ - 90^\circ = 330^\circ$ . If the DAMA annual modulation is due entirely to a stream, its arrival direction on Earth should have ecliptic longitude  $\lambda = 330^\circ \pm 22^\circ$ . Since we use the modulation amplitudes obtained by DAMA assuming a phase such that the maximum rate occurs on June 2, we fix the ecliptic longitude of the arrival direction of the stream at  $\lambda = 340^\circ$ . The amplitude of the modulation depends on the projection of the stream velocity onto the ecliptic, and is proportional to  $\cos \beta_{\text{str}}$ , where  $\beta_{\text{str}}$  is the ecliptic latitude (i.e. the angle above the plane of the ecliptic) of the stream arrival direction.

We let the magnitude of  $\mathbf{v}_{\text{str}}$  vary between  $v_{\text{str}} = 0$  and  $v_{\text{str}} = 1200$  km/s, thus allowing for both Galactic and extragalactic streams (i.e. streams bound or not bound to the Galaxy). A stream is unbound if its Galactocentric speed  $|\mathbf{v}_{\text{str}} + \mathbf{v}_{\odot}|$  exceeds the local escape speed. In formulas, the stream is extragalactic if  $v_{\text{str}} > v_{\odot} \cos \phi + [v_{\text{esc}}^2 - v_{\odot}^2 \sin^2 \phi]^{1/2}$  where  $\cos \phi = \cos \beta_{\text{str}} \cos \beta_{\odot} \cos(\lambda_{\text{str}} - \lambda_{\odot})$ .

Streams bound to our own galaxy have been observed, for example the tidal streams of the Sagittarius dwarf galaxy [22]. The Sagittarius leading tidal stream might pass through or close to the solar neighborhood, with a Galactocentric speed of  $\approx 200$  km/s, but its arrival direction  $(\lambda_{\text{Sgr}}, \beta_{\text{Sgr}}) \approx (187^\circ, 8^\circ)$  does not have the correct ecliptic longitude to give the observed phase of the DAMA modulation without a substantial contribution from the usual halo component. So the stream we are implying should be a different, perhaps yet undiscovered, stream.

There may be dark matter bound not to our galaxy but to our Local Group of galaxies [23], and also dark matter bound to our supercluster, possibly passing through us [19]. A stream made of such dark matter has its Galactocentric incoming speed  $v_{\text{in}}$  at large distances from the Galaxy increased by gravitational focusing while falling into the Galaxy. Its resulting Galactocentric speed near the Sun is  $v_{\text{local}} = \sqrt{v_{\text{in}}^2 + v_{\text{esc}}^2}$ . Its velocity dispersion may increase by a factor  $v_{\text{local}}/v_{\text{in}}$  if the stream self-gravity is negligible, or remain approximately constant in self-gravitating regions of the stream. To give an idea of the Galactocentric velocities involved, a stream with arrival direction  $(\lambda_{\text{str}}, \beta_{\text{str}}) = (340^\circ, 0^\circ)$  and heliocentric speed  $v_{\text{str}} = 800$  km/s requires a local Galactocentric speed  $v_{\text{local}} = 712$  km/s, and, accounting for gravitational focusing, a Galactocentric incoming speed at large distances  $v_{\text{in}} = 293$  km/s. This value is of the same order of magnitude as the Galactic speed relative to the Cosmic Microwave Background (549 km/s, using the CMB dipole measurement in Ref. [24] and the conventional Galactocentric velocity of the Sun in section IV).

The density of an incoming stream is also increased by focusing, at least linearly with the ratio  $v_{\text{local}}/v_{\text{in}}$  (see the argument is Ref. [19]), but possibly by much larger factors, which are however complicated to evaluate. To have a local stream density fraction of the order of a few percent and Galactocentric incoming speeds  $v_{\text{in}} \sim 100$  km/s, the density of the infalling dark matter at infinity must be of the order of the local halo density. This may be possible if a small dark galaxy bound to our supercluster happens to cross our own. Dark matter bound to the Local Group of galaxies is expected to have a much smaller density. The average density of the Local Group of galaxies is of the order of 2.2 times the critical density, i.e.  $0.6 \times 10^{-5} \text{ GeV cm}^{-3}$ , which is only  $2 \times 10^{-5}$  of the local halo density. In order for a stream with say 0.1 of the average density far away from our Galaxy to reach a density of 3% of the local halo density in the solar neighborhood, a focusing enhancement factor of  $1.5 \times 10^4$  is needed. This could only be possible if  $v_{\text{in}}$ , the velocity of the stream with respect to our galaxy, is close to zero, i.e. if the stream or clump of dark matter was initially almost at rest with respect to our Galaxy (in this case  $v_{\text{local}} \simeq v_{\text{esc}}$ ). Moreover, since the velocity dispersion of the stream may be enhanced by a factor of  $10^4$  unless the Solar System happens to be within a self-gravitating region of the stream, the initial velocity dispersion may have to be very small too.

Since the last considerations about an extragalactic stream are rather speculative, we have decided to present results with a wide range of stream velocities, up to 1200 km/s.

To illustrate the effect of a dark matter stream on the allowed WIMP mass and cross section, we take a stream density fraction  $\xi_{\text{str}} = 0.03$  and a stream arrival direction  $(\lambda_{\text{str}}, \beta_{\text{str}}) = (340^\circ, 0^\circ)$  so that the stream is on the plane of the ecliptic. In Figs. 3(a-d), we use the 2-6 and 6-14 keV DAMA bins (the same as in Fig. 2a) to find the region in which the WIMP-proton cross section  $\sigma_p$  at WIMP mass  $m$  reproduces the DAMA annual modulation results at the 90% and  $3\sigma$  C.L. (inner densely hatched region and outer hatched region, respectively). The other lines are experimental upper bounds: the region above each line is excluded at 90% C.L. by the corresponding experiment (DAMA/NaI-96, CRESST-I and II, EDELWEISS, and CDMS-I and II). Notice by comparing Figs. 2 and 3 that the experimental upper limits change when the stream is included. Figs. 3(a-d) correspond to heliocentric speeds of (a) 300 km/s, (b) 600 km/s, (c) 900 km/s, and (d) 1200 km/s. The gaps in the DAMA modulation region in

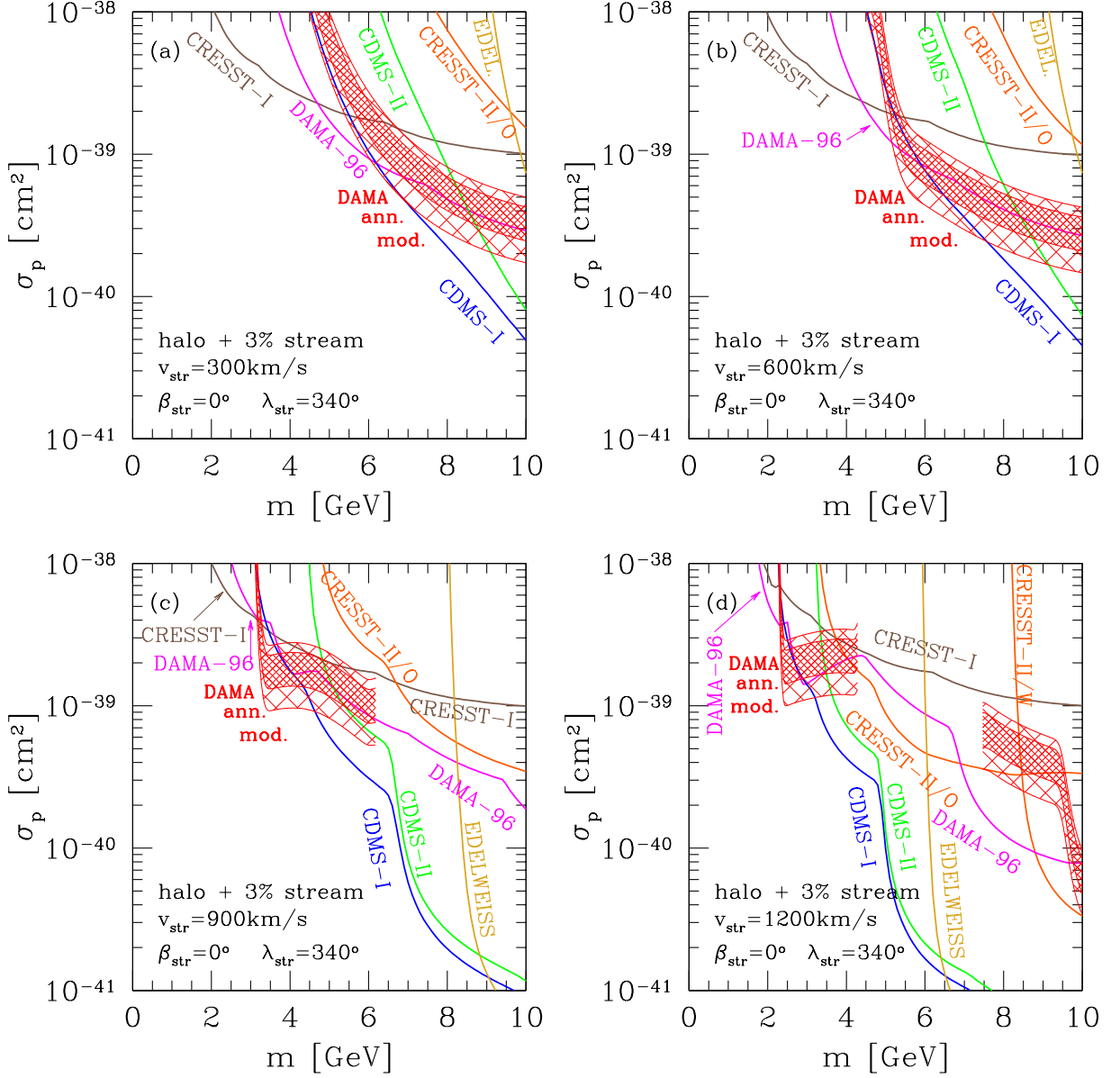


FIG. 3: Same as Fig. 2(a) but with the addition of a dark matter stream with density 3% of the conventional local halo density, heliocentric arrival direction of ecliptic coordinates  $(\lambda_{\text{str}}, \beta_{\text{str}}) = (340^\circ, 0^\circ)$ , and heliocentric speed of (a) 300 km/s, (b) 600 km/s, (c) 900 km/s, and (d) 1200 km/s. The DAMA modulation region is shown both for the 90% and the  $3\sigma$  C.L. (inner densely hatched and outer hatched regions, respectively). The gaps in the DAMA modulation region in panels (c) and (d) are due to our requirement that  $\chi^2_{\text{min}} < 2$ . The experimental upper limits change when the stream is included.

panels (c) and (d) are due to our requirement that  $\chi^2_{\text{min}} < 2$ . We have arbitrarily considered stream velocities up to  $v_{\text{str}} = 1200$  km/s, which is an extremely high velocity, just to show a complete picture. Excluding the highest values of  $v_{\text{str}}$  would eliminate the compatibility region at the lowest WIMP masses.

The range of WIMP masses  $m$  compatible with DAMA and all other experiments is plotted in Figs. 4(a-b) for varying stream heliocentric speeds  $v_{\text{str}}$ . Here we again take a stream density fraction  $\xi_{\text{str}} = 0.03$  and a stream arrival direction  $(\lambda_{\text{str}}, \beta_{\text{str}}) = (340^\circ, 0^\circ)$ . The dashed horizontal lines indicate the heliocentric speed above which the stream must be extragalactic (for the given arrival direction). The inner densely hatched and outer hatched regions correspond to the 90% and  $3\sigma$  C.L., respectively. In Fig. 4(a), we use the 2-6 and 6-14 keVee DAMA bins; in Fig. 4(b), the 2-4 and 6-14 keVee bins. Fig. 4 shows that at the  $3\sigma$  level it is possible to find WIMP masses in the range of 2 to 9 GeV compatible with DAMA and all other experiments at any assumed stream speed.

For different values of the stream density and arrival direction, the results shown in Fig. 4 change. In Figs. 5 and 6



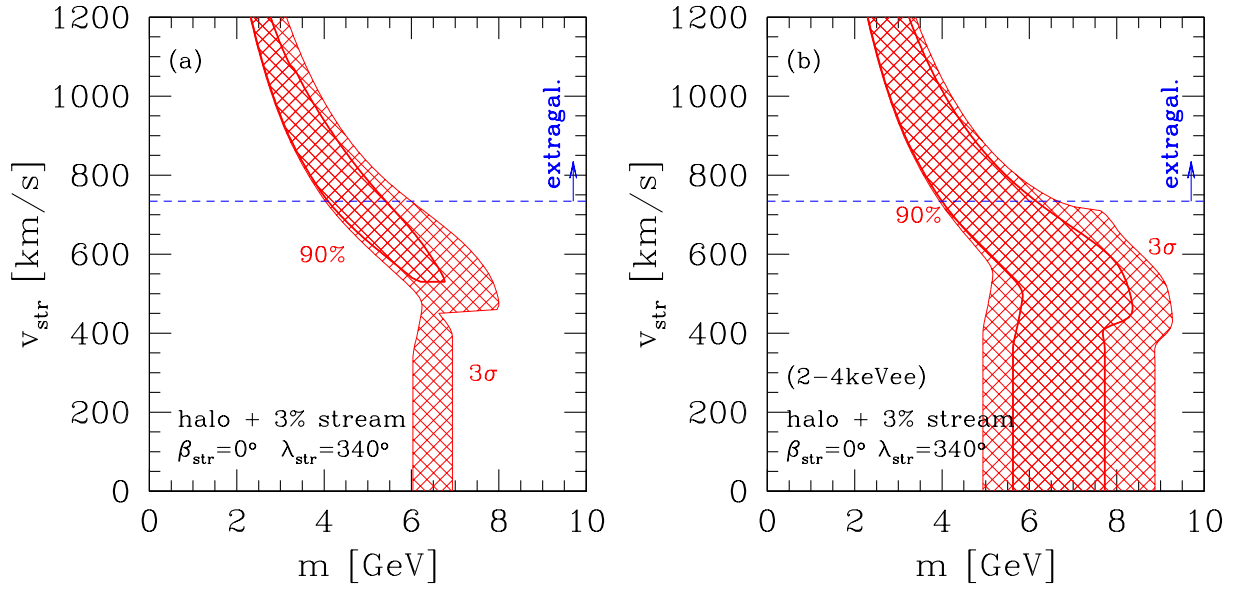


FIG. 4: Range of WIMP masses  $m$  for which there is a compatible region between the DAMA modulation and the other experimental results at various stream heliocentric speeds  $v_{\text{str}}$ . Here the stream is assumed to arrive from ecliptic longitude  $\lambda_{\text{str}} = 340^\circ$  and ecliptic latitude  $\beta_{\text{str}} = 0^\circ$ . Also indicated is the speed above which the stream is extragalactic (dashed horizontal line). The inner densely hatched and outer hatched regions correspond to the 90% and  $3\sigma$  C.L., respectively. In (a), we use the 2-6 and 6-14 keVee DAMA bins; in (b), the 2-4 and 6-14 keVee bins. At the  $3\sigma$  level it is possible to find WIMP masses compatible with DAMA and all other experiments at any assumed stream speed.

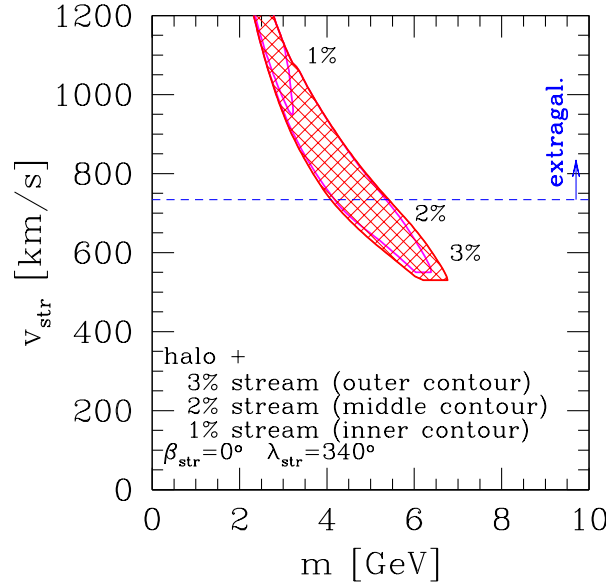


FIG. 5: Same as Fig. 4(a) at the 90% C.L. but showing the effect of changing the stream density from 3% to 2% and to 1% of the local smooth halo density.

we show the variation expected in Fig. 4(a) for the 90% C.L. Similar changes in the size of the compatibility region happen in all other cases considered. In Fig. 5 we show the effect of changing the stream density from 3% to 2% and to 1% of the local smooth halo density. The compatibility region decreases with decreasing stream density. Densities of at least 1% of the local smooth halo density are needed to have a sizable effect. In Fig. 6 we show the effect of changing the stream arrival direction from  $\beta_{\text{str}} = 0^\circ$  to  $\beta_{\text{str}} = 30^\circ$  and to  $\beta_{\text{str}} = 60^\circ$ . For  $\beta_{\text{str}} = 0^\circ$ , the arrival direction of the stream is on the plane of the orbit of the Earth around the Sun, the plane of the ecliptic. For  $\beta_{\text{str}} = 30^\circ$ , the stream

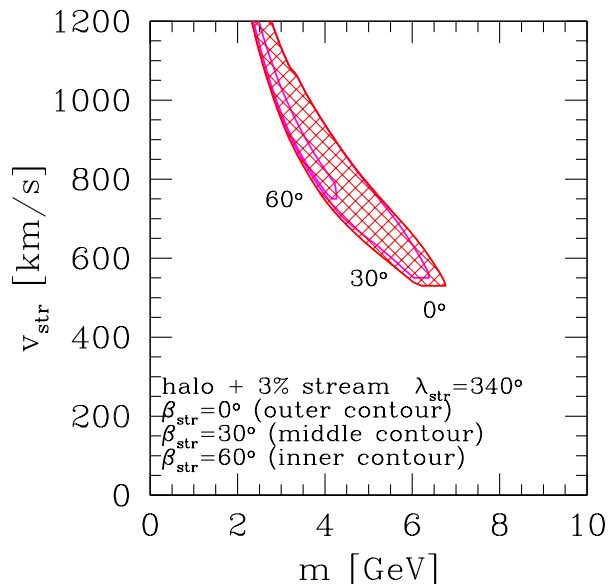


FIG. 6: Same as Fig. 4(a) at the 90% C.L. but showing the effect of changing the stream arrival direction from  $\beta_{\text{str}} = 0^\circ$  to  $\beta_{\text{str}} = 30^\circ$  and to  $\beta_{\text{str}} = 60^\circ$ .

is at  $30^\circ$  of the ecliptic and at  $30^\circ$  of the Sun's Galactocentric velocity. For  $\beta_{\text{str}} = 60^\circ$ , the arrival direction of the stream is aligned with the Sun's Galactocentric velocity. As  $\beta_{\text{str}}$  increases the effect of the stream in the modulation decreases, eventually becoming zero when the stream arrives perpendicularly to the plane of the ecliptic.

## VI. CONCLUSIONS

We have pointed out that for light dark matter particles a signal could be observed by DAMA through its Na, instead of I, component. Such a signal would be below threshold for Ge in CDMS and EDELWEISS. This possibility can be tested with a few months of Si data in CDMS-II, and future O data in CRESST.

For WIMPs with spin independent interactions, we have presented two examples of dark matter velocity distributions that give the annual modulation observed by DAMA but satisfy all other constraints from dark matter searches.

The first is a conventional Maxwellian distribution with a WIMP mass around 5 to 9 GeV. Our results are shown in Fig. 2. This simple possibility remains marginally open. This suggests that if several other possible dark galactic halo models were considered the region of compatibility would be larger.

Our second example is the conventional distribution superposed to a dark matter stream coming from the general direction of the Galactic rotation (but *not* the Sagittarius stream). For the sake of illustration, we have assumed a particular density of the stream (0.03 of the local halo density) and a particular incoming direction (on the plane of the Earth's orbit and the direction of the Sun's velocity in the Galaxy) to obtain the allowed regions presented in Figs. 3 and 4. Figs. 5 and 6 show how the compatibility regions decrease with decreasing stream density and as the direction of arrival of the stream moves away from the plane of the Earth's orbit around the Sun. The effect of the stream is larger (smaller) for larger (smaller) stream densities and for incoming directions closer to (further from) the plane of the Earth's orbit.

For simplicity, we have illustrated our idea only for the case of WIMPs with spin-independent interactions. Other kinds of particles and interactions, or halo velocities distributions more complicated than a conventional Maxwellian distribution, may extend the allowed regions of parameters.

## Acknowledgements

This work was supported in part by the US DOE grant DE-FG03-91ER40662 Task C and NASA grants NAG5-13399

and ATP03-0000-0057.

- 
- [1] For a review, see, e.g., G. Jungman, M. Kamionkowski, and K. Griest, Phys. Rep. **267**, 195 (1996).
  - [2] R. Bernabei *et al.*, Phys. Lett. B **389**, 757 (1996); **424**, 195 (1998); **450**, 448 (1999); **480**, 23 (2000); **509**, 283 (2001); Riv. Nuovo Cim. **26**, 1 (2003); Int. J. Mod. Phys. **D 13**, 2127 (2004); P. Belli *et al.*, Phys. Rev. **D61**, 023512 (2000); Phys. Rev. **D66**, 043503 (2002).
  - [3] A.K. Drukier, K. Freese, and D.N. Spergel, Phys. Rev. **D33**, 3495 (1986); K. Freese, J. Frieman, and A. Gould, Phys. Rev. **D37**, 3388 (1988).
  - [4] D. S. Akerib *et al.* Phys. Rev. **D68**, 082002 (2003); D. Abrams *et al.* Phys. Rev. **D66**, 122003 (2002).
  - [5] D. S. Akerib *et al.* [CDMS Coll.], Phys. Rev. Lett. **93**, 211301 (2004).
  - [6] V. Sanglard [the EDELWEISS Coll.], astro-ph/0306233 (2003).
  - [7] V. Sanglard [the EDELWEISS Coll.], astro-ph/0503265 (2005).
  - [8] J. Jochum *et al.*, Nucl. Phys. Proc. Suppl. **124** (2003) 189; G. Angloher *et al.* Phys. Atom. Nucl. **66** (2003) 494 [Yad. Fiz. **66** (2003) 521].
  - [9] L. Stodolsky, F. Probst, talk at “The Dark Side of the Universe,” Ann Arbor, May 2004.
  - [10] M. Brhlik and L. Roszkowski, Phys. Lett. **B464**, 303 (1999); C.J. Copi and L.M. Krauss, Phys. Rev. **D67**, 103507 (2003); R. Foot, Phys. Rev. **D69**, 036001 (2004); Mod. Phys. Lett. A **19**, 1841 (2004); A.M. Green, Phys. Rev. **D63**, 043005 (2001); Phys. Rev. **D66**, 083003 (2002); Phys. Rev. **D68**, 023004 (2003) Erratum *ibid.* **D69**, 109902 (2004); A. Kurylov and M. Kamionkowski, Phys. Rev. **D69**, 063503 (2004); G. Prézeau, A. Kurylov, M. Kamionkowski, and P. Vogel, Phys. Rev. Lett. **91**, 231301 (2003); C. Savage, P. Gondolo, and K. Freese, Phys. Rev. **D70**, 123513 (2004); D. Smith and N. Weiner, Phys. Rev. **D64**, 043502 (2001); P. Ullio, M. Kamionkowski, and P. Vogel, JHEP 0107, 044 (2001).
  - [11] R. Bernabei *et al.*, Riv. Nuovo Cim. **26**, 1 (2003).
  - [12] A. Gabutti *et al.*, Astropart. Phys. **6**, 1 (1996).
  - [13] A. Bottino, N. Fornengo, and S. Scopel, Phys. Rev. **D67**, 063519 (2003); A. Bottino, F. Donato, N. Fornengo, and S. Scopel, **D68**, 043506 (2003); **D69**, 037302 (2004).
  - [14] R. Bernabei *et al.*, Phys. Lett. **B389**, 757 (1996).
  - [15] S. Eidelman *et al.*, Phys Lett. B **592**, 1 (2004).
  - [16] R.P. Olling and M.R. Merrifield, MNRAS **297**, 943 (1998); *ibid.* **326**, 164 (2001).
  - [17] See e.g. G. Gelmini and P. Gondolo, Phys. Rev. **D64**, 023504 (2001) and references therein.
  - [18] P. Sikivie and J. R. Ipser, Phys. Lett. B **291**, 288 (1992).
  - [19] K. Freese, P. Gondolo and L. Stodolsky, Phys. Rev. **D64**, 123502 (2001).
  - [20] G. Gelmini and P. Gondolo, Phys. Rev. **D64**, 023504 (2001)
  - [21] D. Stiff, L. M. Widrow and J. Frieman, Phys. Rev. **D64**, 083516 (2001).
  - [22] S. R. Majewski *et al.*, Ap. J. **599**, 2082 (2003) H. J. Newberg *et al.* Ap. J. Lett. **596**, 191 (2003); K. Freese, P. Gondolo, H. J. Newberg, and M. Lewis, Phys. Rev. Lett. **92**, 111301 (2004); K. Freese, P. Gondolo, and H. J. Newberg, Phys. Rev. **D71**, 043516 (2005).
  - [23] S. van den Bergh, Astron. Astrophys. Rev. **9**, 273 (1999).
  - [24] C.H. Lineweaver *et al.*, Ap. J. **470**, 38 (1996).
  - [25] S. Courteau and S. van den Bergh, Astron. J. **118** 337 (1999).